Charge-transfer transitions in chromium trihalides

1996 J. Phys.: Condens. Matter 8 8457

(http://iopscience.iop.org/0953-8984/8/44/002)

J. Phys.: Condens. Matter **8** (1996) 8457–8463. Printed in the UK

Charge-transfer transitions in chromium trihalides

K Shinagawa†, H Sato‡, H J Ross§, L F McAven§ and P H Butler§

† Department of Physics, Toho University, Funabashi City, Chiba 274, Japan
‡ Department of Information Science, Ochanomizu University, Bunkyo-ku, Tokyo 112, Japan
§ Department of Physics and Astronomy, University of Canterbury, Christchurch, New Zealand

Received 12 April 1996, in final form 29 July 1996

Abstract. The electronic states of chromium trihalides CrM_3 (M = Cl, Br or I) are calculated by taking a USCF–Xα–SW approach to an assumed $(CrM_6)^{3-}$ octahedral cluster model. It is found that there are three charge-transfer (CT) transitions at the absorption edge. Those transitions are calculated as shifting to lower energies as the halide goes from chlorine to iodine, consistent with the observation. In addition the transition energies obtained from Slater transition state calculations agree well with the observed values. As a result the transitions observed at the absorption band edge are assigned, in energy order, to the CT transitions $4t_{1u}(np) \rightarrow 3e_g(3d)$ and $1t_{2u}(np) \rightarrow 3e_g(3d)$ of π types and $3t_{1u}(np) \rightarrow 3e_g(3d)$ of σ type. Combining this result with the signs of the spin–orbit constants for the CT states, the large Faraday and Kerr rotations observed at the absorption band edge in ferromagnetic $CrBr_3$ can be attributed to the two π-type CT transitions.

1. Introduction

Ferromagnetic materials with a large Faraday or Kerr rotation have been applied to devices such as optical isolators, magnetic sensors and rewritable optical memories [1]. In recent years there has been an increasing demand for materials with large magneto-optical rotation. In order to enhance the magneto-optical rotation, it is important to know the electronic states which give rise to the magneto-optical rotation in each ferromagnetic material. Chromium trihalides are known as typical ferromagnetic materials with large Faraday and Kerr rotations [2].

The optical absorption spectra of chromium trihalides CrM_3 (M = Cl, Br, or I) were first measured by Dillon *et al* [2]. There are many sharp lines and broad bands typical of Cr^{3+} ions in a crystal environment with octahedral symmetry. The positions of the lines and bands were assigned to the crystal-field transitions [2]. In addition to the crystal-field transitions, there appears a strong absorption edge in each absorption spectrum, and the absorption band edge shifts to lower energy as the halide goes from chlorine to iodine. Furthermore, Dillon *et al* [2] measured the absorption spectra in the ferromagnetic state of $CrBr_3$, ($T_c = 36$ K and $4\pi M_s = 3520$ G at $T = 0$ K [2]) and found that the absorption spectra with the magnetization parallel to the *c*-axis differed significantly for the two different circular polarizations. That is, linearly polarized light passing through the magnetic crystal undergoes a rotation of its polarization plane, namely a Faraday rotation. The measured Faraday rotation was over half a million degrees per centimetre at the absorption band edge. Later, Jung [3] measured the Kerr rotation of ferromagnetic $CrBr_3$ in reflection measurements and found a large positive rotation peak at 2.91 eV (23 500 cm^{-1}) and a negative rotation peak at 3.29 eV (26 500 cm^{-1}) of a few degrees. The origin of these large

0953-8984/96/448457+07$19.50

rotations at the absorption band edge was attributed to the charge-transfer (CT) transitions of an electron in the 4p π-type and 4p σ-type orbitals of Br^{-1} to 3d Cr^{3+} orbitals [2, 3]. Recent measurements of the optical properties in the ultraviolet regions, made by Carricaburu *et al* [4] for $CrCl_3$ and by Pollini *et al* [5] for $CrBr_3$, showed that there are three transitions at the absorption band edges. They assigned these transitions to the CT transitions, based on the self-consistent band structures calculated by Antoci and Mihich [6].

The purpose of this paper is to make a definite assignment for the transitions at the absorption band edges in the chromium trihalides, based on the electronic structure calculations, the transition energies of CT transitions, and the spin–orbit constants in the CT states which determine the sign of the Kerr rotation of ferromagnetic $CrBr_3$. In order to calculate the electronic states, we adopt an octahedral $(CrM_6)^{3-}$ cluster model, which for insulators such as CrM_3 (M = Cl, Br or I) is more effective than the band model. To this model we apply an unrestricted self-consistent field (USCF)–Xα–scattering wave (SW) method developed by Johnson and Smith [7]. Larsson and Connolly [8] calculated the electronic states of an octahedral $(CrCl_6)^{3-}$ cluster using the USCF–Xα–SW method and calculated the transferred hyperfine interaction constants to compare with those obtained from ESR experiments. They showed that the transferred hyperfine interaction constants could be explained quite well, although the transition energies of the CT transitions were too small to reproduce those observed by Dillon *et al* [2].

2. USCF–Xα–SW method

The USCF–Xα–SW method is a non-empirical molecular orbital method, in which the one-particle Schrödinger equations are exactly solved numerically with the following approximations. One is that the potential is approximated by a muffin-tin potential. This approximation is less significant for the octahedral cluster treated in this study. The other approximation is that the exchange interaction is approximated by a local statistically averaged exchange multiplied by a factor α [9], which is deduced from the atomic calculations [10]. In the muffin-tin approximation to the potential, the atomic sites are surrounded by non-overlapping spheres and the potential is spherically averaged within these spheres. All the spheres are surrounded by the outer sphere, which touches all the ligand spheres. In the interstitial region, between the atomic spheres, a constant averaged potential is used. In this study, the sphere radii of M^- (M = Cl, Br or I) are assumed to be the ionic radii. In addition, to account for the neighbours of the cluster approximately, we used Watson spheres with the same positive charges as the negative charges of the cluster. The radius of the Watson sphere was assumed to be the same as that of the outer sphere. The parameters used in this study are listed in table 1. Here, it should be noted that our Cr^{3+} radius is different from that adopted by Larsson and Connolly [8] (1.80 au). Furthermore, for simplicity, we assumed that the orbitals except for 3s, 3p and 3d of Cr^{3+} and the highest ns and np of the ligands were the core orbitals in the calculations. The transition energies are calculated using the Slater transition states, where $\frac{1}{2}$ electron is removed from the initial level and added to the final level.

3. Orbital energies and transition energies

The calculated orbital energies of $(CrM_6)^{3-}$ (M = Cl, Br or I) clusters are shown in table 2. Table 3 shows the normalized charge of some orbitals in various regions. The type of each orbital in table 2 was determined by the normalized charge distributions as shown in table 3.

Table 1. Atomic and outer sphere radii and α-values used in the USCF–Xα–SW calculations.

	$(CrCl_6)^{3-}$		$(CrBr_6)^{3-}$		$(CrI_6)^{3-}$	
Cluster	Radius (au)	α	Radius (au)	α	Radius (au)	α
Chromium	1.180	0.7135	1.180	0.7135	1.180	0.7135
Ligand	3.320	0.7233	3.620	0.7061	4.090	0.6987
Outer	7.820	0.7214	8.420	0.7075	9.360	0.7015

Table 2. Orbital energies $-\epsilon$. The numbers in parentheses are the occupation numbers; M and L mean metal and ligand, respectively.

	Orbital	ϵ (Ryd)		
Type	(occupation number)	$(CrCl_6)^{3-}$	$(CrBr_6)^{3-}$	$(CrI_6)^{3-}$
M 4p	$5t_{1u}\downarrow$ (0)	0.0367	0.0329	0.0243
M 4p	$5t_{1u}\uparrow$ (0)	0.0502	0.0450	0.0363
M 4s	$4a_{1g}\downarrow$ (0)	0.1129	0.1094	0.0907
M 4s	$4a_{1g}\uparrow$ (0)	0.1307	0.1257	0.1068
M 3d	$3e_g\downarrow$ (0)	0.1718	0.1677	0.1449
M 3d	$2t_{2g}\downarrow$ (0)	0.1844	0.1781	0.1599
M 3d	$3e_g\uparrow$ (0)	0.4653	0.4613	0.4461
M 3d	$2t_{2g}\uparrow$ (3)	0.4972	0.4911	0.4748
L np	$4t_{1u}\uparrow$ (3)	0.6034	0.6028	0.5432
L np	$1t_{1g}\uparrow$ (3)	0.6613	0.5987	0.5384
L np	$1t_{1g}\downarrow$ (3)	0.6642	0.6018	0.5419
L np	$4t_{1u}\downarrow$ (3)	0.6655	0.6052	0.5459
L np	$2e_g\downarrow$ (2)	0.6817	0.6199	0.5575
L np	$1t_{2u}\uparrow$ (3)	0.7013	0.6428	0.5857
L np	$1t_{2u}\downarrow$ (3)	0.7031	0.6449	0.5883
L np	$2e_g\uparrow$ (2)	0.7046	0.6481	0.5872
L np	$3t_{1u}\uparrow$ (3)	0.7618	0.7087	0.6559
L np	$3t_{1u}\downarrow$ (3)	0.7622	0.7094	0.6579
L np	$1t_{2g}\downarrow$ (3)	0.7697	0.7135	0.6586
L np	$1t_{2g}\uparrow$ (3)	0.7728	0.7167	0.6606
L np	$3a_{1g}\uparrow$ (1)	0.7731	0.7236	0.6740
L np	$3a_{1g}\downarrow$ (1)	0.7740	0.7247	0.6763
L ns	$1e_g\uparrow$ (2)	1.5385	1.4559	1.2085
L ns	$1e_g\downarrow$ (2)	1.5430	1.4610	1.2136
L ns	$2t_{1u}\uparrow$ (3)	1.5505	1.4677	1.2244
L ns	$2t_{1u}\downarrow$ (3)	1.5548	1.4726	1.2295
L ns	$2a_{1g}\uparrow$ (1)	1.5780	1.4937	1.2468
L ns	$2a_{1g}\downarrow$ (1)	1.5819	1.4983	1.2615
M 3p	$1t_{1u}\downarrow$ (3)	3.6254	3.6093	3.5838
M 3p	$1t_{1u}\uparrow$ (3)	3.9642	3.9565	3.9440
M 3s	$1a_{ig}\uparrow$ (1)	5.7559	5.7395	5.7159
M 3s	$1a_{1g}\downarrow$ (1)	6.1049	6.0974	6.0869

From these tables, it is seen that the $3e_g$ and $2t_{2g}$ orbitals correspond to the antibonding orbitals of e_g^* and t_{2g}^* in the ligand field theory [11]. Similarly, $4t_{1u}$, $1t_{2u}$ and $3t_{1u}$ correspond to the non-bonding orbitals of t_{1u}^n (π type), t_{2u}^n (π type) and t_{1u} (σ type), respectively. As the ground state of the cluster is $(t_{2g})^3\ {}^4A_{2g}$, three CT transitions to the excited CT states of $(4t_{1u})^5(3e_g)^1\ {}^4T_{2u}$, $(1t_{2u})^5(3e_g)^1\ {}^4T_{2u}$ and $(3t_{1u})^5(3e_g)^1\ {}^4T_{2u}$ are allowed by the symmetry

Table 3. Normalized electronic charges of some orbitals in various regions.

	Electronic charge			
Orbital	Cr sphere	M sphere	Inter region	Outer region
		$(CrCl_6)^{3-}$		
$3e_g$ ↑	0.6467	0.0379	0.1186	0.0071
↓	0.7098	0.0223	0.1461	0.0101
$2t_{2g}$ ↑	0.7681	0.0082	0.1821	0.0008
↓	0.6995	0.0152	0.2054	0.0040
$1t_{1g}$ ↑	0.0000	0.1603	0.0335	0.0045
↓	0.0000	0.1606	0.0321	0.0043
$4t_{1u}$ ↑	0.0009	0.1578	0.0413	0.0111
↓	0.0009	0.1583	0.0389	0.0105
$1t_{2u}$ ↑	0.0000	0.1575	0.0513	0.0038
↓	0.0000	0.1579	0.0487	0.0036
$2e_g$ ↑	0.1414	0.1330	0.0497	0.0112
↓	0.0251	0.1551	0.0300	0.0140
$3t_{1u}$ ↑	0.0014	0.1558	0.0579	0.0061
↓	0.0016	0.1562	0.0552	0.0059
$1t_{2g}$ ↓	0.0178	0.1498	0.0798	0.0038
↑	0.0036	0.1532	0.0734	0.0037
$3a_{1g}$ ↑	0.0024	0.1585	0.0347	0.0120
↓	0.0026	0.1587	0.0336	0.0117
		$(CrBr_6)^{3-}$		
$3e_g$ ↑	0.5895	0.0515	0.0930	0.0086
↓	0.7049	0.0272	0.1215	0.0104
$2t_{2g}$ ↑	0.7550	0.0136	0.1628	0.0007
↓	0.6713	0.0248	0.1748	0.0049
$1t_{1g}$ ↑	0.0000	0.1600	0.0349	0.0048
↓	0.0000	0.1600	0.0333	0.0046
$4t_{1u}$ ↑	0.0007	0.1573	0.0438	0.0115
↓	0.0009	0.1579	0.0411	0.0109
$1t_{2u}$ ↑	0.0000	0.1580	0.0481	0.0038
↓	0.0000	0.1585	0.0454	0.0035
$2e_g$ ↑	0.1945	0.1246	0.0474	0.0106
↓	0.0244	0.1559	0.0252	0.0150
$3t_{1u}$ ↑	0.0012	0.1576	0.0470	0.0060
↓	0.0014	0.1581	0.0445	0.0058
$1t_{2g}$ ↓	0.0217	0.1507	0.0707	0.0034
↑	0.0021	0.1547	0.0650	0.0034
$3a_{1g}$ ↑	0.0022	0.1604	0.0239	0.0114
↓	0.0026	0.1606	0.0229	0.0111
		$(CrI_6)^{3-}$		
$3e_g$ ↑	0.5381	0.0603	0.0910	0.0091
↓	0.6979	0.0271	0.1299	0.0097
$2t_{2g}$ ↑	0.7524	0.0140	0.1628	0.0005
↓	0.5855	0.0399	0.1563	0.0086
$1t_{1g}$ ↑	0.0000	0.1599	0.0361	0.0048
↓	0.0000	0.1602	0.0342	0.0044
$4t_{1u}$ ↑	0.0006	0.1574	0.0447	0.0104
↓	0.0006	0.1580	0.0416	0.0097
$1t_{2u}$ ↑	0.0000	0.1592	0.0417	0.0034
↓	0.0000	0.1597	0.0387	0.0031
$2e_g$ ↑	0.2455	0.1155	0.0520	0.0095
↓	0.1896	0.1577	0.0195	0.0150
$3t_{1u}$ ↑	0.0009	0.1615	0.0240	0.0059
↓	0.0011	0.1619	0.0217	0.0057
$1t_{2g}$ ↓	0.0230	0.1539	0.0510	0.0027
↑	0.0028	0.1581	0.0459	0.0026
$3a_{1g}$ ↑	0.0017	0.1643	0.0017	0.0108
↓	0.0018	0.1645	0.0008	0.0104

Table 4. Calculated and observed [4, 5] transition energies of CT transitions.

CT transition	Calculated or observed	Transition energy (eV (cm^{-1}))		
		$CrCl_3$	$CrBr_3$	CrI_3
$4t_{1u} \rightarrow 3e_g$	Calculated	4.03 (32 500)	2.82 (22 800)	1.83 (14 800)
	Observed	3.70	2.90	—
$1t_{2u} \rightarrow 3e_g$	Calculated	4.54 (36 600)	3.36 (27 100)	2.41 (19 400)
	Observed	4.75	3.10	—
$3t_{1u} \rightarrow 3e_g$	Calculated	5.35 (43 200)	4.25 (34 300)	3.36 (27 100)
	Observed	5.20	3.80	—

Table 5. Spin–orbit constants in CT states. ζ_{np} is the spin–orbit interaction coefficient of np electron, and S the overlap integral between np orbitals.

CT state	λ
$(4t_{1u})^5(2t_{2g})^3(3e_g)^1\ {}^4T_{2u}$	$-\zeta_{np}/20$
$(1t_{2u})^5(2t_{2g})^3(3e_g)^1\ {}^4T_{2u}$	$\zeta_{np}/20$
$(3t_{1u})^5(2t_{2g})^3(3e_g)^1\ {}^4T_{2u}$	$\zeta_{np}\lvert S\rvert/10$

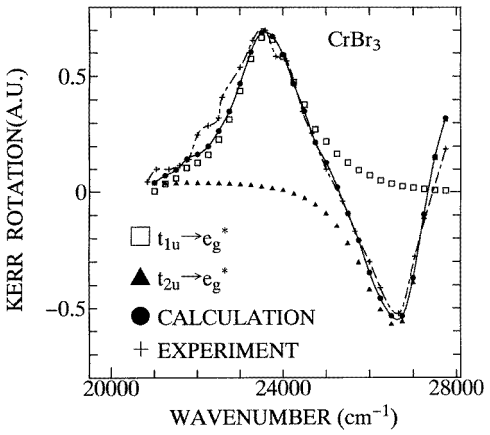

Figure 1. Calculated Kerr rotation spectra at $T = 0$ K and the Kerr rotation spectrum measured by Jung [3] for $CrBr_3$.

consideration. That is, there are three CT transitions from the t_{1u} or t_{2u} ligand level to the unoccupied e_g metal level or $4t_{1u} \rightarrow 3e_g$, $1t_{2u} \rightarrow 3e_g$ and $3t_{1u} \rightarrow 3e_g$. Table 4 shows the transition energies obtained from the Slater transition state calculations, with the observed transition energies measured by Carricaburu *et al* [4] and Pollini *et al* [5]. From this result, it is seen that the calculated transition energies agree well with the observed values, the CT transitions shift to lower energies as the halide goes from chlorine to iodine, consistent with the observations [2, 4, 5] and two π-type CT transitions appear at lower energies. Here, it should be noted that the main reason why the transition energies agree well with the observed values, although those calculated by Larsson and Connolly [8] were too small to be able

to reproduce, may be the different atomic sphere radii that we used in the calculations as mentioned in section 2.

4. Spin–orbit constants in charge-transfer states

The allowed CT states in CrM_3 (M = Cl, Br or I) are $\{(t_{1u})^5(t_{2g})^3(e_g)^1\}\ ^4T_{2u}$ for $4t_{1u} \rightarrow 3e_g$ and $3t_{1u} \rightarrow 3e_g$, and $\{(t_{2u})^5(t_{2g})^3(e_g)^1\}\ ^4T_{2u}$ for $1t_{2u} \rightarrow 3e_g$. As the ground state is $^4A_{2g}$, the Faraday or Kerr effect in ferromagnetic CrM_3 originates from the spin–orbit constants of the excited CT states [2, 12]. That is, the larger the spin–orbit constant, the larger the Faraday or Kerr rotation becomes, and the sign of the rotation corresponds to the sign of the spin–orbit constant.

The spin–orbit constant of the CT state is defined by [2]

$$\lambda = \langle\{(t_{1u} \text{ or } t_{2u})^5(t_{2g})^3(e_g)^1\}^4T_{2u} \parallel V_{SO} \parallel \{t_{1u} \text{ or } t_{2u})^5(t_{2g})^3(e_g)^1\}^4T_{2u}\rangle / \langle S \parallel S \parallel S\rangle \times \langle^4T_2 \parallel L \parallel {}^4T_2\rangle$$

$$\langle S \parallel S \parallel S\rangle = \{S(S+1)(2S+1)\}^{1/2}$$

$$\langle^4T_2 \parallel L \parallel {}^4T_2\rangle = (6)^{1/2}i.$$

The reduced matrix element of the spin–orbit interaction V_{SO} can be calculated using the Wigner–Racah calculus [2] or using the RACAH software developed at the University of Canterbury in New Zealand [13]. The results are shown in table 5. Here, it should be noted that the signs of λ differ in the first two CT states, contrary to the previous study [2]. This means that the Kerr rotation, which originates from the two CT transitions, must have an opposite sign consistent with the observation [3]. Furthermore, it should be noted that the spin–orbit constant in the third CT state is smaller than those of others by an order of magnitude owing to the overlap integral S. As Dillon *et al* [2] suggested, these π-type transitions are important for the Faraday or Kerr rotation at the absorption edge, although the absorption strengths are too weak to observe. To check this assignment further, we tried to calculate the Kerr rotation spectrum using the Kerr rotation dispersion formula and the optical data measured by Jung [3]. The Kerr rotation spectra calculated by assuming the transition energies in table 4 and $\zeta_{4p} = 2460\ cm^{-1}$ [12] are shown in figure 1 with the observed Kerr rotation spectrum [13]. It is seen that the observed Kerr rotation spectrum could be reproduced quite well. So, we can assign the transitions at the absorption band edges in chromium trihalides, which are related to the large Faraday or Kerr rotation, to the CT transitions $4t_{1u} \rightarrow 3e_g$ and $1t_{2u} \rightarrow 3e_g$ of π type.

5. Summary and conclusions

The electronic states of the chromium trihalides CrM_3 (M = Cl, Br or I) were calculated using the USCF–Xα–SW method [7] based on the $(CrM_6)^{3-}$ octahedral cluster model. Slater transition state calculations were carried out to obtain the transition energies of the allowed transitions, which were compared with the observed energies. In addition, the spin–orbit constants of the CT states were calculated using the RACAH software [3], thus determining the sign of the Kerr rotation. From the result of these calculations, we present the following conclusions.

(1) There are three CT transitions at the absorption band edges, consistent with the observations [4, 5]. Two of those are assigned to π-type transitions and one to a σ-type transition. These CT transitions shift to lower energies as the halide goes from chlorine

to iodine, consistent with the observations [2, 4, 5], and the transition energies of the CT transitions agree well with the observed values.

(2) Owing to the transition energies of the CT transitions, and the signs of spin–orbit constants, the two CT transitions of π type, namely $4t_{1u} \rightarrow 3e_g$ and $1t_{2u} \rightarrow 3e_g$, are seen to give rise to large Faraday or Kerr rotations observed at the absorption band edge in ferromagnetic $CrBr_3$.

(3) The transitions at the absorption band edges in CrM_3 (M = Cl, Br or I) were assigned, in energy order, to the CT transitions $4t_{1u} \rightarrow 3e_g$ and $1t_{2u} \rightarrow 3e_g$ of π type and $3t_{1u} \rightarrow 3e_g$ of σ type.

References

[1] Dillon J F Jr 1990 *J. Magn. Magn. Mater.* **84** 213
[2] Dillon J F Jr, Kamimura H and Remeika J P 1962 *Phys. Rev. Lett.* **9** 161; 1966 *J. Phys. Chem. Solids* **27** 1531
[3] Jung W 1965 *J. Appl. Phys.* **36** 2422
[4] Carricaburu B, Ferre J, Mamy R, Pollini I and Thomas J 1986 *J. Phys.: Solid State Phys.* **19** 4985
[5] Pollini I, Thomas J, Carricaburu B and Mamy R 1989 *J. Phys.: Condens. Matter* **1** 7695
[6] Antoci S and Mihich L 1978 *Phys. Rev.* B **18** 5768
[7] Johnson K H and Smith F C 1972 *Phys. Rev.* B **5** 831
[8] Larsson S and Connolly J W D 1974 *J. Chem. Phys.* **60** 1514
[9] Slater J C 1951 *Phys. Rev.* **82** 538
[10] Schwartz K 1972 *Phys. Rev.* B **5** 2466
[11] Sugano S, Tanabe Y and Kamimura H 1970 *Multiplets of the Transition Metal Ions in Crystals* (New York: Academic)
[12] Shinagawa K, Suzuki T, Saito T and Tsushima T 1995 *J. Magn. Magn. Mater.* **140–4** 171
[13] Ross H J, McAven L F, Shinagawa K and Butler P H 1996 *J. Comput. Phys.* **128**